International Journal of Control

ISSN: 0020-7179 (Print) 1366-5820 (Online) Journal homepage: https://www.tandfonline.com/loi/tcon20

Observer based fault reconstruction schemes using terminal sliding modes

Mohammad Mousavi, Mostafa Rahnavard & Shadi Haddad

To cite this article: Mohammad Mousavi, Mostafa Rahnavard & Shadi Haddad (2018): Observer based fault reconstruction schemes using terminal sliding modes, International Journal of Control, DOI: 10.1080/00207179.2018.1487082

To link to this article: https://doi.org/10.1080/00207179.2018.1487082

Accepted author version posted online: 10 Jun 2018.
Published online: 19 Jul 2018.

INTERNATIONAL JOURNAL OF CONTROL
https://doi.org/10.1080/00207179.2018.1487082

Taylor & Francis
Taylor & Francis Group

Observer based fault reconstruction schemes using terminal sliding modes

Mohammad Mousavi, Mostafa Rahnavard and Shadi Haddad

School of Mechanical Engineering, College of Engineering, University of Tehran, Tehran, Iran

ABSTRACT

Two state/fault estimation methods using terminal sliding mode (TSM) concepts are presented in this paper. In contrast with conventional sliding modes, which guarantee asymptotic convergence of non-output estimation errors and faults, TSMs enable finite time convergence of estimation errors for faults and all the states. The minimum-phase condition, as a common condition required for fault estimation, is released in the proposed methods. *Method I* implements fractional power of the so-called switching term to make it robust against matched faults and disturbances. Compared with previous terminal scheme, this method covers a wider class of systems. In *Method II*, fractional power sliding variable is considered to achieve finite time convergence of estimation errors and their derivatives. In contrast with *Method I*, this approach is also robust against unmatched faults. Finally, the methods are applied to an unstable aircraft model.

ARTICLE HISTORY
Received 3 August 2017
Accepted 28 May 2018

KEYWORDS
Sliding mode observer; terminal sliding modes; fault reconstruction; finite time convergence

1. Introduction

Fault reconstruction and estimation (FRE) schemes are used to increase safety, reliability and maintainability and provide the information about magnitude and shape of fault which are very useful for fault tolerant control. Sliding mode concepts have been exploited in many researches to design observers and controllers (Chua, Tan, Aldeen, & Saha, 2017; Halim, Edwards, & Tan, 2011; Kee, Tan, Ng, & Trinh, 2014; Ooi, Tan, Chua, & Wang, 2017; Ooi, Tan, Nurzaman, & Ng, 2017; Plestan, Shtessel, Bregeault, & Poznyak, 2010; Rahnavard, Hairi Yazdi, & Ayati, 2017; Shtessel, Edwards, Fridman, & Levant, 2014; Yang & Zhu, 2013). Sliding mode observers (SMOs) have been widely used for FRE in recent years. This is due to their robustness to disturbances and modelling uncertainties and capability of estimating unknown inputs (Ng, Tan, Ng, & Trinh, 2015, 2016; Rahnavard, Ayati, & Hairi Yazdi, 2018; Ríos, Punta, & Fridman, 2017; Tan & Edwards, 2003; Tan, Crusca, & Aldeen, 2008; Utkin, 1992; Wang, Tan, & Zhou, 2017; Yan & Edwards, 2007). Linear observers only guarantee asymptotic convergence of output estimation error. SMOs enable the output estimation error to converge to zero in finite time, while non-output states estimation error will converge to zero asymptotically, meaning that the error states converge to zero in time of infinity (Edwards, Spurgeon, & Patton, 2000; Tan, Yu, & Man, 2010).

Terminal sliding mode (TSM) concepts enable the finite time convergence of both measured and unmeasured states' estimation errors (Al-Ghanimi, Zheng, & Man, 2017; Mousavi, Rahnavard, Hairi Yazdi, & Ayati, 2018; Su, 2017; Wei & Guo, 2009; Zhihong & Yu, 1997; Zuo, 2015). A terminal sliding mode controller (TSMC) was developed in Park and Tsuji (1999) for an uncertain second-order system. Yu and Zhihong (2002) proposed a fast TSM controller for single-input-single-output linear dynamical systems. In S. Yu, X. Yu, Shirinzadeh, and Man (2005) TSM concept was used to provide a continuous-time finite-time control method for robotic manipulators, which enhances the tracking performance. Wei and Guo (2009) proposed a novel type of control scheme combining the disturbance-observer-based control with TSM control for a class of multiple-input–multiple-output continuous nonlinear systems subject to disturbances. By integrating disturbance-observer-based control with TSM control laws, the disturbances can be rejected and attenuated and the desired dynamic performances can be guaranteed in finite time. Wang et al. (2017) developed a novel SMO for systems that do not satisfy common conditions required for FRE, in particular the so-called matching condition and minimum-phase condition.

In Tan et al. (2010) a terminal sliding mode observer (TSMO) is proposed for a certain class of nonlinear systems. They introduced a non-smooth discontinuous injection term including fractional powers in the observer which guarantees finite time convergence of all non-output error states. The system under consideration is n-degree-of-freedom with measurable position and unmeasurable velocity states, which results in a special state space representation. In Chu and Zhang (2014) thruster fault of an underwater autonomous vehicle (UAV) is reconstructed based on the TSMO proposed in Tan et al. (2010).

From the literature it is concluded that a few works have been published regarding to the estimation of faults in finite time. In Tan et al. (2010) the authors did not consider any fault and the proposed observer only estimates the states. In fact, in the case that a fault occurs in the system the convergence of observer is not guaranteed. Furthermore, the considered system is very special and satisfaction of minimum-phase condition is required. In Chu and Zhang (2014) the actuator fault is estimated in finite time for an UAV, which has the special structure of system considered in Tan et al. (2010).

CONTACT Mostafa Rahnavard m.rahnavard@ut.ac.ir

Compared with the current literature, this paper considers the systems with general linear state space representation affected by faults and disturbances. The proposed observers are robust against matched and unmatched faults/disturbances and can estimate all of states and matched faults/disturbances in finite time. The unmatched disturbances have no effect on reconstruction of faults. The minimum-phase condition is a common condition required for fault estimation (Chu & Zhang, 2014; Halim et al., 2011; Tan et al., 2010; Tan & Edwards, 2003, 2010; Wang et al., 2017). This condition could be stringent and limit the applicability of fault reconstruction. This condition is no longer required in this paper and the system can be non-minimum-phase.

In more detail, two state/fault estimation methods using TSM concepts and fractional power signals are presented. *Method I* proposes a TSMO, which makes use of fractional powers and injects an additional non-smooth discontinuous switching term to the conventional observer. Hereby, matched faults/disturbances are estimated in finite time. Compared with previous terminal scheme, this method covers a wider class of systems. In *Method II*, fractional power sliding variable is considered to achieve finite time convergence of estimation errors and their derivatives. Compared to *Method I*, this approach is robust against matched and unmatched faults. The effects of unmatched faults/disturbances are rejected in matched fault reconstruction. Rigorous mathematical proofs are presented for both methods. Finally, an unstable aircraft model is considered for simulations to compare the performance of proposed methods with together and conventional SMO.

This paper is structured as follows. Section 2 proposes a design procedure for terminal SMOs in addition to convergence proofs. Section 3 presents a simulation example and Section 4 concludes the paper.

2. Methodology

2.1 Method I: state/fault estimation using fractional power of switching function

Consider a time-invariant linear system as

$$\begin{aligned} \dot{x}(t) &= Ax(t) + Bu(t) + Ff(t), \\ y(t) &= Cx(t). \end{aligned} \tag{1}$$

$f(t) \in \boldsymbol{R}^q$ represents faults, disturbances, or nonlinearities. $A \in \boldsymbol{R}^{n\times n}$, $B \in \boldsymbol{R}^{n\times m}$, $C \in \boldsymbol{R}^{p\times n}$, and $F \in \boldsymbol{R}^{n\times q}$ are system matrices. It is assumed that $||f(t)|| \leq \gamma_1$ and also the system is observable. The proposed TSMO has the structure of

$$\begin{aligned} \dot{\hat{x}}(t) &= A\hat{x}(t) + Bu(t) + G_1 e_y(t) + G_2 \nu(t) + G_3 \nu^{\frac{\alpha}{\beta}}, \\ \hat{y}(t) &= C\hat{x}(t). \end{aligned} \tag{2}$$

where $e_y(t) = \hat{y}(t) - y(t)$ is output estimation error, α and β ($\alpha < \beta$) are odd integers, and $\nu(t) \in \boldsymbol{R}^p$ is a vector containing discontinuous switching terms with the structure $\nu(t) = [\nu_1 \ \nu_2 \ \cdots \ \nu_p]^{\mathrm{T}}$, and $\nu_i = sign(e_{2,i})$. e_2 is defined later. The observer of *Method I* estimates the states and faults in finite time if:

$\boldsymbol{A}_1$. $rank(CF) = rank(F) = q$

$\boldsymbol{A}_2$. $2p \geq n + q$

A change of coordinates $Tx(t) \to \bar{x}(t)$ is defined to provide the system matrices in the following structure:

$$\begin{aligned} &\bar{A} = \begin{bmatrix} A_1 & A_2 \\ A_3 & A_4 \end{bmatrix}, A_3 = \begin{bmatrix} A_{31} \\ A_{32} \end{bmatrix}, \bar{B} = \begin{bmatrix} B_1 \\ B_2 \end{bmatrix}, \bar{F} = \begin{bmatrix} F_1 \\ F_2 \end{bmatrix}, \\ &\bar{C} = \begin{bmatrix} 0 & C_2 \end{bmatrix}, \end{aligned} \tag{3}$$

$A_1 \in \boldsymbol{R}^{(n-p)\times(n-p)}$, $A_3 \in \boldsymbol{R}^{p\times(n-p)}$, $A_{31} \in \boldsymbol{R}^{(n-p)\times(n-p)}$, $F_1 \in \boldsymbol{R}^{(n-p)\times q}$, $F_2 \in \boldsymbol{R}^{p\times q}$. $C_2 \in \boldsymbol{R}^{p\times p}$ is full rank. A_{31} is full rank since the system is supposed to be observable (Tan & Edwards, 2003). In the new coordinates we have $\bar{x}^{\mathrm{T}} = [\bar{x}_1^{\mathrm{T}} \quad \bar{x}_2^{\mathrm{T}}]$ and $y = C_2\bar{x}_2$. $\bar{x}_1$ and $\bar{x}_2$ denote non-output and output states, respectively. As definitions, $e_1 = \widehat{\bar{x}}_1 - \bar{x}_1$ and $e_2 = \widehat{\bar{x}}_2 - \bar{x}_2$ are non-output and output estimation errors. Subtracting (2) from (1) and transforming to the new coordinates, yields:

$$\begin{aligned} \dot{e}_1(t) &= A_1 e_1(t) + A_2 e_2(t) + L_1 C_2 e_2(t) + L_2 \nu(t) \\ &\quad + L_3 \nu^{\frac{\alpha}{\beta}} - F_1 f(t), \\ \dot{e}_2(t) &= A_3 e_1(t) + A_4 e_2(t) + L_4 C_2 e_2(t) + L_5 \nu(t) - F_2 f(t), \end{aligned} \tag{4}$$

The observer gains are designed in the new system and then transformed to the system of (1).

$$G_1 = T^{-1}\begin{bmatrix} L_1 \\ L_4 \end{bmatrix}, G_2 = T^{-1}\begin{bmatrix} L_2 \\ L_5 \end{bmatrix}, G_3 = T^{-1}\begin{bmatrix} L_3 \\ 0 \end{bmatrix}. \tag{5}$$

Proposition 2.1: *There exist matrices L_1 and L_4 to stabilise $Z = \begin{bmatrix} A_1 & A_2+L_1C_2 \\ A_3 & A_4+L_4C_2 \end{bmatrix}$.*

Proof: Choose $L_1 = -\mathrm{A}_2C_2^{-1} + A_{2s}C_2^{-1}$ and $L_4 = -A_4C_2^{-1} + A_{4s}C_2^{-1}$, where $A_{2s} \in \boldsymbol{R}^{(n-p)\times p}$ and $A_{4s} \in \boldsymbol{R}^{p\times p}$ are design matrices. Substituting into Z gives $Z = \begin{bmatrix} A_1 & A_{2s} \\ A_3 & A_{4s} \end{bmatrix}$. Now, the problem is to stabilise Z with suitable choice of A_{2s} and A_{4s}. Consider a transformation in the form of $T_{zw} = \begin{bmatrix} I_{n-p} & M \\ 0 & I_p \end{bmatrix}$, where $M \in \boldsymbol{R}^{(n-p)\times p}$ will be designed in the following. Transforming of Z gives:

$$W = T_{zw}ZT_{zw}^{-1} = \begin{bmatrix} W_1 & W_2 \\ W_3 & W_4 \end{bmatrix}, \tag{6}$$

where $W_1 = A_1 + MA_3$, $W_2 = -A_1M - MA_3M + A_{2s} + MA_{4s}$, $W_3 = A_3$, and $W_4 = A_{4s} - A_3M$.

A_3 is full column rank since the system is detectable. Therefore, there exists M such that $W_1 < 0$. Then, choose A_{4s} to stabilise W_4 and A_{2s} to hold $W_2 = 0$. In mathematics:

$$\begin{cases} M : A_1 + MA_3 < 0 \\ A_{4s} : A_{4s} - A_3M < 0 \\ A_{2s} = A_1M + MA_3M - MA_{4s} \end{cases}. \tag{7}$$

By substituting (7) into (6), $W = \begin{bmatrix} W_1<0 & 0 \\ W_3 & W_4<0 \end{bmatrix}$. In this structure, the eigen values of W are the union of eigen values of W_1 and W_4 which are negative. It means that even for a fully unstable system, which satisfies $\boldsymbol{A}_2$, there exist L_1 and L_4 such that $Z < 0$. ■

Proposition 2.2: *Define $L_5 = -\rho I_p$, where ρ is a positive scalar and is determined in proposition 2.3. Then for the error system (4), $e(t)$ is bounded in finite time.*

Proof: The error system of Equation (4) can be rewritten as:

$$\dot{e} = Ze + \begin{bmatrix} L_2 \\ L_5 \end{bmatrix} \nu + \begin{bmatrix} L_3 \\ 0 \end{bmatrix} \nu^{\frac{\alpha}{\beta}} - Ff, \tag{8}$$

where $Z = \begin{bmatrix} A_1 & A_2+L_1C_2 \\ A_3 & A_4+L_4C_2 \end{bmatrix} < 0$ from *proposition 2.1*. Define a Lyapunov function as $V_0 = \frac{1}{2}e^{\mathrm{T}}e$. Taking the derivative gives:

$$\dot{V}_0 = e^{\mathrm{T}}\dot{e} = e^{\mathrm{T}}Ze + e^{\mathrm{T}} \begin{bmatrix} L_2\nu + L_3\nu^{\frac{\alpha}{\beta}} \\ L_5\nu \end{bmatrix} - e^{\mathrm{T}}Ff. \tag{9}$$

Applying Rayleigh's inequality to the first term and using Cauchy–Schwarz inequality (Tan & Edwards, 2003) for the other terms of (9) results in:

$$\dot{V}_0 < -||e||(\mu||e|| - (||L_2||\sqrt{p} + \rho\sqrt{p} + ||F||\gamma_1 + ||L_3||\sqrt{p})), \tag{10}$$

where p is the number of outputs and $\mu = -\lambda_{max}(Z)$. If $||e|| > \frac{\sqrt{p}(||L_2||+||L_3||+\rho)+||F||\gamma_1}{\mu}$, then $\dot{V}_0 < 0$. Defining $R = \sqrt{p}(||L_2|| + ||L_3|| + \rho) + ||F||\gamma_1/\mu$, this implies that $||e||$ is bounded by the ball of radius R (i.e. $||e|| \leq R$).

Consider the ball of radius $R' = R + \varepsilon$, where ε is an arbitrary positive scalar. The error $e(t)$ is bounded by the ball of radius R' in finite time. Assume that $||e|| > R'$, then $\dot{V}_0 < -\mu\varepsilon\sqrt{2V_0}$. Denote $V_0(0)$ and t_0 as the initial value of Lyapunov function and the time of convergence to the ball of R'. Then it stands: $t_0 < \frac{(\sqrt{2V_0(0)}-(R+\varepsilon))}{\mu\varepsilon}$ and the proof is complete. ■

Proposition 2.3: *$e_2(t)$ converges to zero in finite time by appropriate choice of ρ.*

Proof: Consider the Lyapunov function $V_2(t) = \frac{1}{2}e_2^{\mathrm{T}}(t)e_2(t)$. Then,

$$\dot{V}_2 = e_2^{\mathrm{T}}\dot{e}_2 = e_2^{\mathrm{T}}(A_3e_1 + A_4e_2 + L_4C_2e_2 + L_5\nu - F_2f) \tag{11}$$

$$\begin{aligned}\dot{V}_2 &= e_2^{\mathrm{T}}A_{4s}e_2 + e_2^{\mathrm{T}}A_3e_1 - \rho e_2^{\mathrm{T}} \\ &\quad \times [sign(e_{2,1}) \quad sign(e_{2,2}) \quad \ldots \quad sign(e_{2,p})]^{\mathrm{T}} - e_2^{\mathrm{T}}F_2f \\ &< ||e_2||\{||A_3e_1|| - \rho + ||F_2||\gamma_1\}.\end{aligned}$$

For a positive scalar of η_1, $\dot{V}_2 < -\eta_1||e_2||$ if $\rho > ||A_3e_1|| + ||F||_2\gamma_1 + \eta_1$ (see *Remark 2.1*). Using the fact that $V_2(t) = \frac{1}{2}||e_2||^2$, it holds

$$\frac{dV_2}{2\sqrt{V_2}} < -\frac{\eta_1}{\sqrt{2}}dt. \tag{12}$$

Define t_2 as the time taken V_2 equals zero. Integrating (12) and setting $V_2(t_2) = 0$, gives $t_2 < {\eta_1}^{-1}\sqrt{2V_2(0)}$. Thus $e_2(t)$ converges to zero in the finite-time 't_2' and the proof is complete.

Once $e_2(t)$ converges to zero, the error system is reduced as following:

$$\begin{aligned}\dot{e}_1 &= A_1e_1 + L_3\nu_{S_2}^{\frac{\alpha}{\beta}} + L_2\nu_{S_2} - F_1f, \\ 0 &= A_3e_1 - \rho\nu_{S_2} - F_2f,\end{aligned} \tag{13}$$

where $\nu_{S_2}(t)$ is the equivalent switching term when $e_2(t) = 0$.

Consider $\nu_{S_2} = \begin{bmatrix} \nu_1 \\ \nu_2 \end{bmatrix}$ and $F_2 = \begin{bmatrix} 0 \\ F_{22} \end{bmatrix}$, where $\nu_1 \in \boldsymbol{R}^{(n-p)}$, $\nu_2 \in \boldsymbol{R}^{(2p-n)}$, $F_{22} \in \boldsymbol{R}^{(2p-n)\times q}$. From the second part of (13) it is concluded: $\nu_1 = \rho^{-1}A_{31}e_1$. Consider L_2 and L_3 with the special structure of $L_2 = [L_{21}L_{22}]$ and $L_3 = [L_{31}0]$, where $L_{21} \in \boldsymbol{R}^{(n-p)\times(n-p)}$, $L_{22} \in \boldsymbol{R}^{(n-p)\times(2p-n)}$, and $L_{31} \in \boldsymbol{R}^{(n-p)\times(n-p)}$. From the first part of (13), it is concluded:

$$\begin{aligned}\dot{e}_1(t) &= (A_1 + \rho^{-1}L_{21}A_{31} + \rho^{-1}L_{22}A_{32})e_1 \\ &\quad - (F_1 + \rho^{-1}L_{22}F_{22})f + \rho^{-\frac{\alpha}{\beta}}L_{31}(A_{31}e_1)^{\frac{\alpha}{\beta}}.\end{aligned} \tag{14}$$

Define $\hat{A}_1 = A_1 + \rho^{-1}L_{21}A_{31} + \rho^{-1}L_{22}A_{32}$. For eliminating the effect of f in (14) and stabilising $\hat{A}_1$, L_{21} and L_{22} are chosen such that

$$\begin{aligned}L_{22}F_{22} &= -\rho F_1 \\ L_{21} &= -(\rho k_0 + \rho A_1 + L_{22}A_{32})A_{31}^{-1},\end{aligned} \tag{15}$$

where k_0 is an arbitrary positive scalar. Thus, (14) is simplified as $\dot{e}_1 = -k_0e_1 + \rho^{-\frac{\alpha}{\beta}}L_{31}(A_{31}e_1)^{\frac{\alpha}{\beta}}$.

Define $\bar{e}_1(t) = A_{31}e_1(t)$, $\bar{e}_1 \in \boldsymbol{R}^{n-p}$. Multiplying $\dot{e}_1$ by A_{31} from left hand side gives:

$$\dot{\bar{e}}_1 = -k_0\bar{e}_1 + \rho^{-\frac{\alpha}{\beta}}A_{31}L_{31}\bar{e}_1^{\frac{\alpha}{\beta}}. \tag{16}$$

■

Proposition 2.4: *$e_1(t)$ converges to zero in finite time by choice of $L_{31} = -\sigma\rho^{\frac{\alpha}{\beta}}A_{31}^{-1}$, where σ is an arbitrary positive scalar.*

Proof: Substituting L_{31} in (16) gives:

$$\dot{\bar{e}}_1 = -k_0\bar{e}_1 - \sigma\bar{e}_1^{\frac{\alpha}{\beta}}. \tag{17}$$

Consider a Lyapunov function as $\bar{V}_1(t) = \bar{e}_1^{\mathrm{T}}(t)\bar{e}_1(t)$. The time-derivative of $\bar{V}_1$ is derived as:

$$\dot{\bar{V}}_1 = -2k_0\bar{e}_1^{\mathrm{T}}\bar{e}_1 - 2\sigma\bar{e}_1^{\mathrm{T}}\bar{e}_1^{\frac{\alpha}{\beta}}. \tag{18}$$

It is obvious that $-2k_0\bar{e}_1^{\mathrm{T}}\bar{e}_1$ is negative definite, So

$$\dot{\bar{V}}_1 < -2\sum_{i=1}^{n-p}\sigma\bar{e}_{1,i}^{\frac{\alpha+\beta}{\beta}}. \tag{19}$$

Then, it stands:

$$\dot{\bar{V}}_1 < -2\sigma\sum_{i=1}^{n-p}(\bar{e}_{1,i}^2)^{\frac{(\alpha+\beta)}{2\beta}}. \tag{20}$$

Since $\alpha < \beta$, it holds: $\frac{(\alpha+\beta)}{2\beta} < 1$ and $\bar{V}_1^{\frac{(\alpha+\beta)}{2\beta}} = (\sum_{i=1}^{n-p}\bar{e}_{1,i}^2)^{\frac{(\alpha+\beta)}{2\beta}} < \sum_{i=1}^{n-p}(\bar{e}_{1,i}^2)^{\frac{(\alpha+\beta)}{2\beta}}$. Thus,

$$\dot{\bar{V}} < -2\sigma\bar{V}_1^{\frac{(\alpha+\beta)}{2\beta}}. \tag{21}$$

Assume $\bar{V}_1(0)$ as the initial value of $\bar{V}_1$ (when the sliding motion is achieved on $e_2 = 0$) and t_1 as the time taken for $\bar{V}_1$ to converge to zero. Integrating both sides of (21) results in:

$t_1 < \frac{\beta}{\sigma(\beta-\alpha)}\bar{V}_1^{(\beta-\alpha)/2\beta}(0)$. This implies that $e_1(t) = A_{31}^{-1}\bar{e}_1(t)$ will converge to zero in finite time and this completes the proof.

Consider $\nu_{S_1} = \begin{bmatrix} \nu_1 \\ \nu_2 \end{bmatrix}$ as the equivalent injection term when the sliding motion takes place on $e_1(t) = 0, e_2(t) = 0$. Continuous approximation of ν_{S_1} can be obtained by passing ν through a low-pass filter or by replacing $\nu_i = sign(e_{2,i})$ with $\nu_i = \frac{e_{2,i}}{|e_{2,i}|+\delta}$, where δ is a small positive scalar (Edwards et al., 2000; Utkin, 1992).

From (13), the fault signal is reconstructed as:

$$\hat{f}(x,t) = -\rho(F_{22}^{\mathrm{T}}F_{22})^{-1}F_{22}^{\mathrm{T}}\nu_2. \tag{22}$$

■

Remark 2.1: The condition $\rho > ||A_3e_1|| + ||F_2||\gamma_1 + \eta_1$ from *proposition 2.3* is simplified as $\rho > \frac{\bar{\eta}}{1-\kappa}$ where $\bar{\eta}$ and κ are defined as: $\bar{\eta} = \eta_1 + ||A_3||\varepsilon + ||F_2||\gamma_1 + \frac{||A_3||||F||\gamma_1}{\mu}$ and $\kappa = \frac{\sqrt{p}||A_3||(1+\sigma||A_{31}^{-1}||+k_0||A_{31}^{-2}||+||A_1A_{31}^{-1}||+(1+||A_{32}A_{31}^{-1}||)||F_{22}||||F_1||||(F_{22}^{\mathrm{T}}F_{22})^{-1}||)}{\mu}$. Since $||e||_1 \leq ||e||$, from *proposition 2.2* it holds: $||e||_1 \leq (R+\varepsilon)$. Using the well-known inequality $||A_3e_1|| \leq ||A_3||||e_1||$, $\rho > ||A_3e_1|| + ||F_2||\gamma_1 + \eta_1$ can be rewritten as: $\rho > \eta_1 + ||A_3||(R+\varepsilon) + ||F_2||\gamma_1$. Replacing R from *proposition 2.1* and with respect to the definitions of L_2 and L_3, it is concluded that: $\rho > \frac{\bar{\eta}}{1-\kappa}$. Note that μ should be chosen large enough to ensure that: $\kappa < 1$.

Finally, the design algorithm of TSMO of *Method I* is summarised as follows. Find a transformation matrix T to achieve the structure in (3). Then determine L_1 and L_4 from *proposition 2.1*, L_5 from *proposition 2.2* and *Remark 2.1*, L_2 from (15), and L_3 from *proposition 2.4*. Fault signal is also reconstructed from (22). Use (5) to transform the design matrices to the original coordinate.

2.2 Method II: state/fault estimation using fractional power sliding variable

Method II collaborates with the observer structure of (2), but fractional power signal is not used (i.e. $L_3 = G_3 = 0$). Moreover, all states can be prone to faults and finite time state estimation is not corrupted in case that $2p \geq n$. Consider the observable system of (1) with $||f(t)|| \leq \gamma_1$ and $||\dot{f}(t)|| \leq \gamma_2$. Assume γ_1 and γ_2 are known. Using an orthogonal transformation (Tan et al., 2008), f can be partitioned to unmatched ($f_1 \in R^{q_1}$) and matched ($f_2 \in R^{q_2}$) parts, i.e. $Ff = \begin{bmatrix} F_1f_1 \\ F_2f_2 \end{bmatrix}$. The error system becomes:

$$\begin{aligned} \dot{e}_1 &= A_1e_1 + A_2e_2 + L_1C_2e_2 + L_2\nu - F_1f_1, \\ \dot{e}_2 &= A_3e_1 + A_4e_2 + L_4C_2e_2 + L_5\nu - F_2f_2. \end{aligned} \tag{23}$$

If the conditions $\boldsymbol{B}_1$ and $\boldsymbol{B}_2$ are satisfied, then the errors e_1 and e_2 converge to zero in finite time and f_2 is reconstructed.

$\boldsymbol{B}_1$: $2p \geq n$

Once $e_1 = e_2 = 0$ occurs, those faults satisfying the matching condition $\boldsymbol{B}_2$ are reconstructed in finite time.

$\boldsymbol{B}_2$: $rank(CF) = rank(F_2)$

According to *propositions 2.1-2.3*, for any non-minimum system, $||e|| \leq R$ and e_2 converges to zero in finite time. In other words, the procedures to prove that $||e||$ is bounded and e_2 converge to zero in finite time are similar to *Method I*. Then, it follows that:

$$\begin{aligned} \dot{e}_1 &= A_1e_1 + L_2\nu_{S_2} - F_1f_1, \\ 0 &= A_3e_1 - \rho\nu_{S_2} - F_2f_2. \end{aligned} \tag{24}$$

From $\boldsymbol{B}_1$, there exists $A_{31} \in R^{(n-p)\times(n-p)}$ as a full rank partition in A_3. (24) is rewritten in the form of:

$$\rho\begin{bmatrix} \nu_1 \\ \nu_2 \end{bmatrix} = \begin{bmatrix} A_{31} \\ A_{32} \end{bmatrix}e_1 - \begin{bmatrix} F_{21} \\ F_{22} \end{bmatrix}f_2,$$

$$\nu_1 = \rho^{-1}(A_{31}e_1 - F_{21}f_2). \tag{25}$$

Proposition 2.5: *e_1 converges to zero in finite time by choice of $L_2 = [-\sigma A_{31}^{-1} \quad 0]$, where σ is a positive scalar.*

Proof: The structure of L_2 means that $\dot{e}_1 = A_1e_1 + L_{21}\nu_1 - F_1f_1$ and the proposed observer uses ν_1 to push e_1 toward zero. Consider that the discontinuous version of the switching term is employed in *Method II*. Define a sliding variable $s = \dot{e}_1 + m_0e_1^{\frac{\alpha}{\beta}}$, and a Lyapunov function $V_1 = \frac{1}{2}s^{\mathrm{T}}s$. Consider (26)-(32) as the preliminaries of the proof.

$$\dot{\nu}_1 = \rho^{-1}A_{31}A_1e_1 + \rho^{-1}A_{31}L_{21}\nu_1 - \rho^{-1}A_{31}F_1f_1, \tag{26}$$

$$\frac{d}{dt}\left(m_0e_1^{\frac{\alpha}{\beta}}\right) = m_0\left[diag\left(e_{1,i}^{\frac{\alpha}{\beta}-1}\right)\right]\dot{e}_1, \quad i = 1,2\ldots n-p, \tag{27}$$

$$\begin{aligned} ||\dot{e}||_1 \leq{}& (||A||_1 + \rho^{-1}||L_{21}A_{31}||)R \\ &+ (||F||_1 + \rho^{-1}||L_{21}F_{21}||)\gamma_1 : \Pi_1, \end{aligned} \tag{28}$$

$$||s|| \leq \Pi_1 + m_0R^{\frac{\alpha}{\beta}} : \Pi_2, \tag{29}$$

$$\left\|\frac{d}{dt}\left(m_0e_1^{\frac{\alpha}{\beta}}\right)\right\| \leq \Pi_1m_0R^{\frac{\alpha}{\beta}-1} : \Pi_3. \tag{30}$$

Substituting the structure of L_2 gives:

$$\Pi_1 = (\rho^{-1}||A_{31}^{-1}F_{21}||\gamma_1 + R\rho^{-1})\sigma + R||A_1|| + \gamma_1||F_1||, \tag{31}$$

$$\begin{aligned} \ddot{e}_1 &= (A_1 + \rho^{-1}L_{21}A_{31})A_1e_1 - A_1F_1f_1 - \rho^{-1}L_{21}A_{31}F_1f_1 \\ &\quad - F_1\dot{f}_1 - \rho^{-1}L_{21}F_{21}\dot{f}_2 + A_1L_{21}\nu_1 + \rho^{-1}L_{21}A_{31}L_{21}\nu_1 \\ &= (A_1 - \sigma\rho^{-1}I_{n-p})A_1e_1 - A_1F_1f_1 + \sigma\rho^{-1}F_1f_1 - F_1\dot{f}_1 \\ &\quad + \sigma\rho^{-1}A_{31}^{-1}F_{21}\dot{f}_2 - \sigma A_1e_1 \\ &\quad + \sigma A_1A_{31}^{-1}F_{21}f_2 + \sigma^2\rho^{-1}A_{31}^{-1}\nu_1. \end{aligned} \tag{32}$$

The time-derivative of V_1 is:

$$\begin{aligned} \dot{V}_1 = s^{\mathrm{T}}\dot{s} = s^{\mathrm{T}}\Big\{&(A_1 - \sigma\rho^{-1}I_{n-p})A_1e_1 - A_1F_1f_1 \\ &+ \sigma\rho^{-1}F_1f_1 - F_1\dot{f}_1 + \sigma\rho^{-1}A_{31}^{-1}F_{21}\dot{f}_2 - \sigma A_1e_1 \\ &+ \sigma A_1A_{31}^{-1}F_{21}f_2 + \sigma^2\rho^{-1}A_{31}^{-1}\nu_1 + \frac{d}{dt}\left(m_0e_1^{\frac{\alpha}{\beta}}\right)\Big\} \end{aligned}$$

$$\dot{V}_1 = s^{\mathrm{T}}\Big\{(A_1 - \sigma\rho^{-1}I_{n-p})A_1e_1 - A_1F_1f_1 + \sigma\rho^{-1}F_1f_1 - F_1\dot{f}_1 + \sigma\rho^{-1}A_{31}^{-1}F_{21}\dot{f}_2 - \sigma A_1e_1 + \sigma A_1A_{31}^{-1}F_{21}f_2 + \frac{d}{dt}\left(m_0e_1^{\frac{\alpha}{\beta}}\right)\Big\} + \sigma^2\rho^{-1}s^{\mathrm{T}}A_{31}^{-1}v_1. \quad (33)$$

Expanding the last term of (33) results in:

$$s^{\mathrm{T}}A_{31}^{-1}v_1 = (A_1e_1 - F_1f_1 + m_0e_1^{\frac{\alpha}{\beta}})^{\mathrm{T}}A_{31}^{-1}v_1 - \sigma v_1^{\mathrm{T}}(A_{31}^{-1})^{\mathrm{T}}A_{31}^{-1}v_1 \quad (34)$$

Substituting (34) into (33) gives:

$$\dot{V}_1 = s^{\mathrm{T}}\Big\{(A_1 - \sigma\rho^{-1}I_{n-p})A_1e_1 - A_1F_1f_1 + \sigma\rho^{-1}F_1f_1 - F_1\dot{f}_1 + \sigma\rho^{-1}A_{31}^{-1}F_{21}\dot{f}_2 - \sigma A_1e_1 + \sigma A_1A_{31}^{-1}F_{21}f_2 + \frac{d}{dt}\left(m_0e_1^{\frac{\alpha}{\beta}}\right)\Big\} + \sigma^2\rho^{-1}(A_1e_1 - F_1f_1 + m_0e_1^{\frac{\alpha}{\beta}})^{\mathrm{T}}A_{31}^{-1}v_1 - \sigma^3\rho^{-1}v_1^{\mathrm{T}}(A_{31}^{-1})^{\mathrm{T}}A_{31}^{-1}v_1. \quad (35)$$

Using Cauchy–Schwarz inequality, Π_4 is defined as the upper bound of $\dot{V}_1$. Then,

$$\begin{aligned}\dot{V}_1 < {} & \Pi_2\{(||A_1^2|| + \sigma\rho^{-1}||A||_1 + \sigma||A_1||)R \\ & + (||A_1F||_1 + \sigma\rho^{-1}||F_1|| + \sigma||A_1A_{31}^{-1}F_{21}||)\gamma_1 \\ & + (||F||_1 + \sigma\rho^{-1}||A_{31}^{-1}F_{21}||)\gamma_2 + \Pi_3\} \\ & + \sigma^2\rho^{-1}(||A_1||R + ||F_1||\gamma_1 + m_0R^{\frac{\alpha}{\beta}}) \\ & - \sigma^3\rho^{-1}v_1^{\mathrm{T}}(A_{31}^{-1})^{\mathrm{T}}A_{31}^{-1}v_1 : \Pi_4. \end{aligned} \quad (36)$$

Note that $(A_{31}^{-1})^{\mathrm{T}}A_{31}^{-1}$ is a symmetric positive definite matrix and $\lambda_{\min}$ is its minimum eigen value. According to the Rayleigh inequality, $v_1^{\mathrm{T}}(A_{31}^{-1})^{\mathrm{T}}A_{31}^{-1}v_1 \geq \lambda_{\min}||v_1||^2 = (n-p)\lambda_{\min}$. Hence, $-\sigma^3\rho^{-1}v_1^{\mathrm{T}}(A_{31}^{-1})^{\mathrm{T}}A_{31}^{-1}v_1 \leq \sigma^3\rho^{-1}(n-p)\lambda_{\min}$. To achieve $V_1 = 0$ in finite time, σ should be adjusted such that $\dot{V}_1 < -\eta_2||s||$. Substituting (29) and (36) as the upper bounds of $||s||$ and $\dot{V}_1$, it is obvious that $\dot{V}_1 + \eta_2||s|| < \Pi_4 + \eta_2\Pi_2$. We need to prove $\Pi_4 + \eta_2\Pi_2 < 0$ in the following.

$$\begin{aligned}& \Pi_2\{(||A_1^2|| + \sigma\rho^{-1}||A_1|| + \sigma||A_1||)\Pi_1 \\ & + (||A_1F_1|| + \sigma\rho^{-1}||F||_1 + ||\sigma A_1A_{31}^{-1}F_{21}||)\gamma_1 \\ & + (||F||_1 + \sigma\rho^{-1}||A_{31}^{-1}F_{21}||)\gamma_2 + \Pi_3 + \eta_2\} \\ & + \sigma^2\rho^{-1}(||A_1||R + ||F_1||\gamma_1 + m_0R^{\frac{\alpha}{\beta}}) \\ & - \sigma^3\rho^{-1}v_1^{\mathrm{T}}(A_{31}^{-1})^{\mathrm{T}}A_{31}^{-1}v_1 \\ & < \Pi_2\{(||A_1^2|| + \sigma\rho^{-1}||A_1|| + \sigma||A_1||)\Pi_1 \\ & + (||A_1F||_1 + \sigma\rho^{-1}||F||_1 + \sigma||A_1A_{31}^{-1}F_{21}||)\gamma_1 \\ & + (||F_1|| + \sigma\rho^{-1}||A_{31}^{-1}F_{21}||)\gamma_2 + \Pi_3 + \eta_2\} \\ & + \sigma^2\rho^{-1}(||A_1||R + ||F_1||\gamma_1 + m_0R^{\frac{\alpha}{\beta}}) \\ & - \sigma^3\rho^{-1}(n-p)\lambda_{min} = g(\sigma, \sigma^2, \sigma^3). \end{aligned} \quad (37)$$

For a wide range in the choice of σ, $g(\sigma)$ is negative, since it is a cubic polynomial. Therefore, convergence of V_1 to zero occurs in $t_1 < \eta_2^{-1}\sqrt{2V_1(0)}$. Consequently, if $s = 0$, in $t_{e1} < \frac{\beta}{m_0(\beta-\alpha)}e_1(0)^{1-\frac{\alpha}{\beta}}$ convergence of e_1 is established.

With respect to *propositions 2.3* and *2.5*, e_1 and e_2 converge to zero in finite time. Finally, using a low-pass filter on the switching term, f_2 is estimated from (24) as:

$$\hat{f}_2 = -(F_2^{\mathrm{T}}F_2)^{-1}F_2^{\mathrm{T}}\rho v_{filt}. \quad (38)$$

Method II is summarised as follows. Find the transform T to achieve the structure in (3). Then, determine L_1 and L_4 from *proposition 2.1*, L_5 from *proposition 2.2* and *Remark 2.1*, and L_2 from *proposition 2.5*. Revert the design matrices to the original system coordinate using (5). ■

Remark 2.2: Consider the case that there exists disturbance uncertainty in the faulty system. The fault and disturbance signals can be combined to create a new augmented fault vector (Tan et al., 2008). Then, the methodology of paper can be applied to estimate the augmented fault. In the case of matched disturbance, the fault and disturbance both are estimated in finite time. But in the case of unmatched disturbance, only the fault is estimated and the effect of disturbance is rejected. Moreover, consider the situation that faults occur in system sensors. A new state vector, which is filtered version the corrupted outputs, is defined. By defining an augmented state vector, which is the combination of system states and new states, an augmented state space system can be represented (Tan & Edwards, 2003). In the augmented system, the sensor faults are regarded as actuator faults and the methodology of paper can be implemented to estimate the sensor faults.

3. Simulation and results

Example 3.1: A non-minimum phase aircraft model (Narendra & Tripathi, 1973) is simulated in this example. V_x, V_y, θ, and $\dot{\theta}$ are system states which represent horizontal velocity, vertical velocity, pitch angle, and pitch rate, respectively. This model consists of collective and longitudinal pitch systems as actuators. The aim is to compare state estimations and fault reconstruction quality of *Method I*, *Method II* and conventional sliding mode. The third sensor is corrupted by a fault signal $f_s(t)$. The system matrices are:

$$A_0 = \begin{bmatrix} -0.0366 & 0.0271 & -0.4555 & 0.0188 \\ 0.0482 & -1.01 & -4.0208 & 0.0024 \\ 0 & 0 & 0 & 1 \\ 0.1002 & 0.3681 & 1.42 & -0.707 \end{bmatrix},$$

$$B_0 = \begin{bmatrix} 0.4422 & 0.1761 \\ 3.5446 & -7.5922 \\ 0 & 0 \\ -5.52 & 4.49 \end{bmatrix}, \quad C_0 = \begin{bmatrix} 1 & 0 & 0 & 0 \\ 0 & 1 & 0 & 0 \\ 0 & 0 & 1 & 0 \end{bmatrix}.$$

As stated in *Remark 2.2*, a virtual dynamic is constructed for the faulty sensor and it is augmented with the main system. The filter gain is $\Omega = 0.1$. The augmented matrices A, B, C, and F

are:

$$A = \begin{bmatrix} A_0 & 0_{4\times1} \\ [0,0,\Omega,0] & -\Omega \end{bmatrix}, \quad B = \begin{bmatrix} B_0 \\ 0 \end{bmatrix},$$
$$C = \begin{bmatrix} 1 & 0 & 0 & 0 & 0 \\ 0 & 1 & 0 & 0 & 0 \\ 0 & 0 & 0 & 0 & 1 \end{bmatrix}, \quad F = \begin{bmatrix} 0 & 0 & 0 & 0 & \Omega \end{bmatrix}^{\mathrm{T}}.$$

In this case, $n = 5$, $p = 3$, and $q = 1$. The conditions $\boldsymbol{A}_1, \boldsymbol{A}_2$ from *Method 1* and $\boldsymbol{B}_1, \boldsymbol{B}_2$ from *Method 2* are satisfied. Also, V_x and V_y are output states, while θ and $\dot{\theta}$ are non-output states. Regarding to the structure of (3), the transformation matrix T and the transformed matrices are:

$$T = \begin{bmatrix} 0 & 0 & 1 & 0 & 0 \\ 0 & 0 & 0 & 1 & 0 \\ 1 & 0 & 0 & 0 & 0 \\ 0 & 1 & 0 & 0 & 0 \\ 0 & 0 & 0 & 0 & 1 \end{bmatrix}, \quad F_1 = F_{21} = \begin{bmatrix} 0 \\ 0 \end{bmatrix}, \quad F_2 = \begin{bmatrix} 0 \\ 0 \\ 0.1 \end{bmatrix}.$$

From *proposition 2.1*, A_{2s}, A_{4s}, and M are adjusted so that $Z < 0$. A_1 is unstable, since its eigen values are 0.889 and -1.596.

$$A_3 = \begin{bmatrix} -0.455 & 0.0188 \\ -4.021 & 0.0024 \\ 0.01 & 0 \end{bmatrix}, \quad A_{31} = \begin{bmatrix} -0.455 & 0.0188 \\ -4.021 & 0.0024 \end{bmatrix},$$
$$C_2 = I_3, \quad M = \begin{bmatrix} 1000 & 0 & 0 \\ 0 & 1000 & 0 \end{bmatrix}, \quad A_{4s} = -500 I_3,$$
$$\rho = 10, \quad \eta_1 = 5.$$

Design matrices for each method are illustrated in the following. The values of gains L_1, L_4, and L_5 are similar in both methods for more reliable comparison. All the states are initially at unity with proper dimensions. The other observers' parameters are as:

- *Method I*: $L_2 = \begin{bmatrix} -0.322 & 2.524 & 0 \\ -539.7 & 61.14 & 0 \end{bmatrix}$, $L_3 = \begin{bmatrix} -0.0322 & 0.2524 & 0 \\ -53.97 & 6.114 & 0 \end{bmatrix}$, $\alpha = 1$, $\beta = 3$, $P_1 = I_2$.
- *Method II*: $L_2 = \begin{bmatrix} 650 & 0.2524 & 0 \\ -53.97 & 6.114 & 0 \end{bmatrix}$, $L_3 = 0$, $\eta_2 = 10$.
- Conventional sliding mode: $L_2 = 0$, $L_3 = 0$.

Figures 1–3 illustrate fault and state estimation. Both proposed methods present suitable performance, while the conventional method diverges, since A_1 is unstable. Output and non-output estimation errors are shown in Figure 4. From *proposition 2.2*, $||e||$ becomes bounded in finite time. Also, from *propositions 2.4, 2.4*, and *2.5*, $||e_1||$ and $||e_2||$ should converge to zero in less than 2.1s and 0.4s for *Method I* and 1.9s and 0.4s for *Method II*. As demonstrated in Figure 4, it is obvious that the expectations of *propositions 2.2-2.5* are achieved.

Example 3.2: In this example, the performance of *Method II* is examined on aircraft model of Example 3.1. The model is prone to four actuator faults as: $f^{\mathrm{T}} = [f_1 f_2 f_3 f_4]$ with $F = I_4$. Note that f_1 is a step function, f_2 is integral of white noise, f_3 and f_4 are sinusoid functions. In this case, $n = q = 4$ and $p = 3$. From *proposition 2.5*, f_1, f_2 and f_3 should be estimated in finite time. f_4 is unmatched and the observer is robust against it. For $T = \begin{bmatrix} [0001] \\ C_0 \end{bmatrix}$ some of transformed matrices

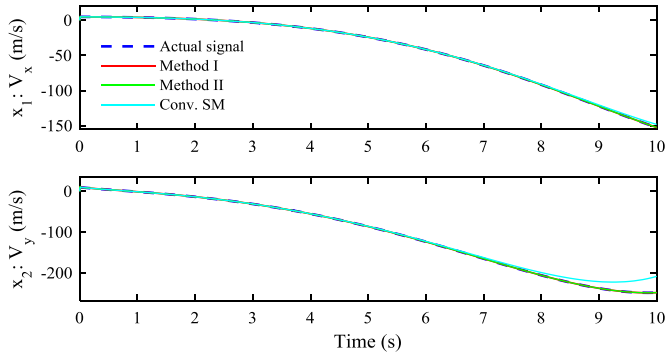

Figure 1. Output-state estimation: V_x, V_y.

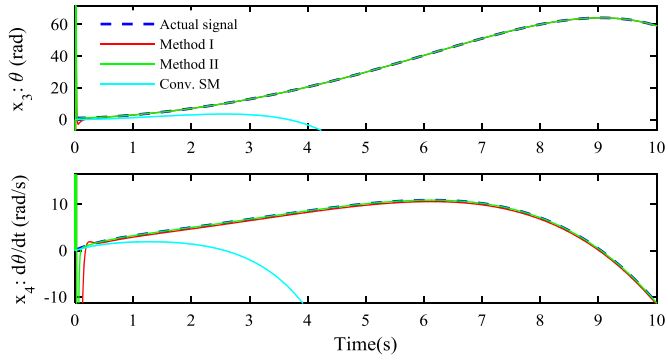

Figure 2. Non-output-state estimations: $\theta, \dot{\theta}$.

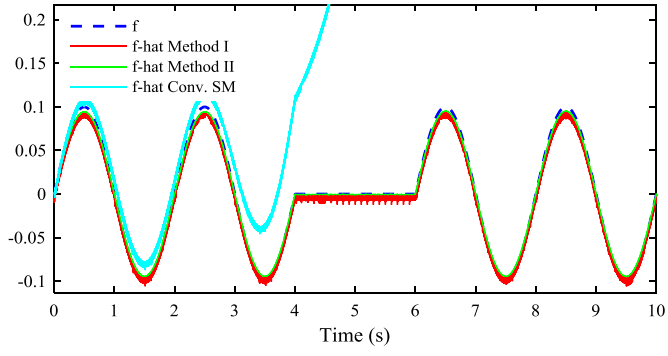

Figure 3. Fault estimation. Actual signal is dashed.

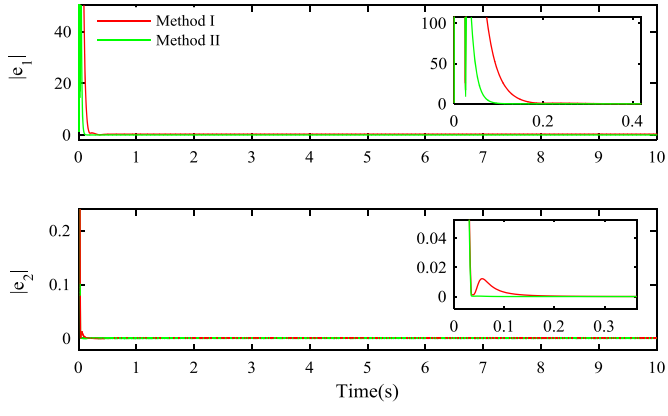

Figure 4. Norms of output and non-output estimation errors.

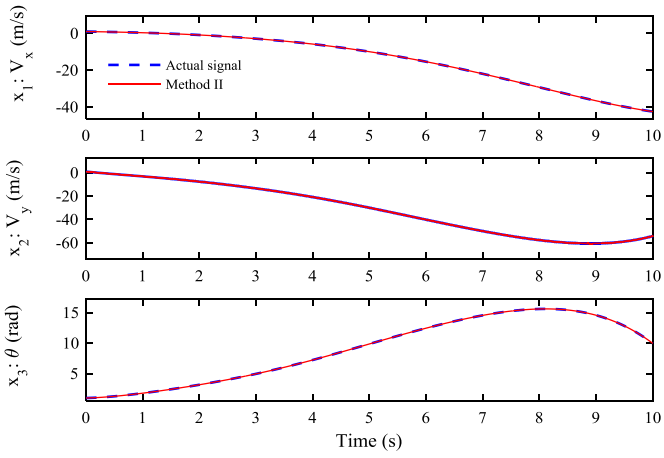

Figure 5. Output-state estimation: V_x, V_y, and θ.

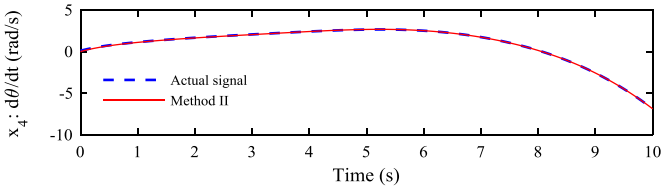

Figure 6. Non-output-state estimation $\dot{\theta}$.

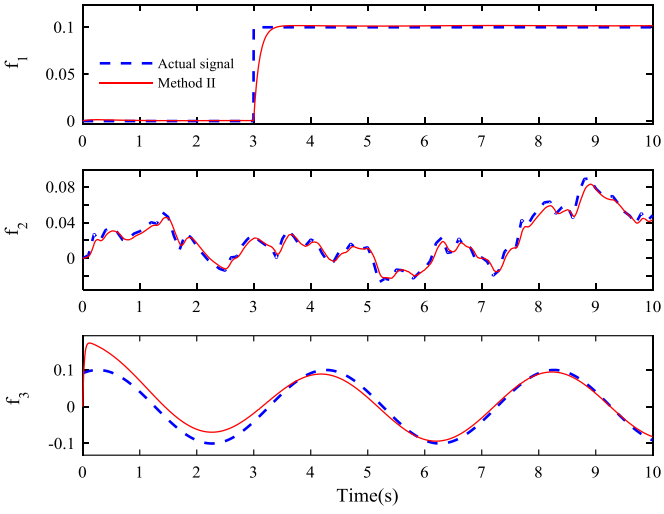

Figure 7. Fault estimation using *Method II*.

are: $A_1 = [-0.707]$, $A_3 = [0.01880.00241]^{\mathrm{T}}$, $A_{31} = [1]$, $F_1 = [1000]$. $F_{21} = [0001]$.

In the transformed system, the first state is non-output and the others are output states. The design matrices are introduced as:

$L_1 = [\,-0.1\ \ -0.3\ \ -4.99e4\,]$, $L_2 = [\,-80\ 0\ 0\,]$, $\rho = 50$, $A_{4s} = -500I_3$. Figures 5–7 reveal that the states and faults are estimated faithfully by the proposed observer.

4. Conclusion

This paper proposes two terminal SMOs as *Method I* and *Method II*. Finite time state/fault estimation and release of the minimum-phase condition are the main characteristics of proposed observers. The effectiveness of the methods is verified by implementation on an unstable aircraft model. Compared with the existing terminal observers, *Method I* (Observer 1) estimates the matched faults and generalises terminal SMOs for wider class of systems satisfying a necessary condition. *Method II* (Observer 2), as a distinct approach, considers fractional power sliding variables to achieve finite time convergence of estimation errors. In addition to finite time convergence of non-output estimation error, its derivative is also forced toward zero. This is due to the fractional power manner of sliding variable and can be considered as the novelty of the second method. *Method II* (Observer 2) is robust against unmatched bounded faults and also incorporates a less restrict condition compared with *Method I* (Observer 1). However, there exist some limitations that can be considered as perspectives. In *Method I*, the number of faults for estimation is restricted by a necessary condition. Moreover noise effects can be considered and decoupled in measurements and estimations using adaptive filters.

Disclosure statement

No potential conflict of interest was reported by the authors.

References

Al-Ghanimi A., Zheng J., & Man Z. (2017). A fast non-singular terminal sliding mode control based on perturbation estimation for piezoelectric actuators systems. *International Journal of Control*, *90*(3), 480–491.

Chua, W.S., Tan, C.P., Aldeen, M., & Saha, S. (2017). A robust fault estimation scheme for a class of nonlinear systems. *Asian Journal of Control*, *19*(2), 799–804.

Chu, Z.-Z., & Zhang, M.-J. (2014). Fault reconstruction of thruster for autonomous underwater vehicle based on terminal sliding mode observer. *Ocean Engineering*, *88*, 426–434.

Edwards, C., Spurgeon, S.K., & Patton, R.J. (2000). Sliding mode observers for fault detection and isolation. *Automatica*, *36*, 541–553.

Halim, A., Edwards, C., & Tan, C.P. (2011). *Fault detection and fault-tolerant control using sliding modes*. *Springer Science & Business Media*.

Kee, C.Y., Tan, C.P., Ng, K.Y., & Trinh, H. (2014). New results in robust functional state estimation using two sliding mode observers in cascade. *International Journal of Robust and Nonlinear Control*, *24*(15), 2079–2097.

Mousavi, M., Rahnavard, M., Hairi Yazdi, M.R., & Ayati, M. (2018). On the Development of Terminal Sliding Mode Observers. In *26th Iranian Conference on Electrical Engineering (ICEE2018)*, IEEE.

Narendra, K.S., & Tripathi, S. (1973). Identification and optimization of aircraft dynamics. *Journal of Aircraft*, *10*(4), 193–199.

Ng, J.Y., Tan, C.P., Ng, K.Y., & Trinh, H. (2015). New results in common functional state estimation for two linear systems with unknown inputs. *International Journal of Control, Automation and Systems*, *13*(6), 1538–1543.

Ng, J.Y., Tan, C.P., Trinh, H., & Ng, K.Y. (2016). A common functional observer scheme for three systems with unknown inputs. *Journal of the Franklin Institute*, *353*(10), 2237–2257.

Ooi, J.H.T., Tan, C.P., Chua, W.-S., & Wang, X. (2017). State and unknown input estimation for a class of infinitely unobservable descriptor systems using two observers in cascade. *Journal of the Franklin Institute*, *354*(18), 8374–8397.

Ooi, J.H.T., Tan, C.P., Nurzaman, S.G., & Ng, K.Y. (2017). A sliding mode observer for infinitely unobservable descriptor systems. *IEEE Transactions on Automatic Control*, *62*(7), 3580–3587.

Park, K.B., & Tsuji, T. (1999). Terminal sliding mode control of second order nonlinear uncertain systems. *International Journal of Robust and Nonlinear Control*, *9*, 769–780.

Plestan, F., Shtessel, Y., Bregeault, V., & Poznyak, A. (2010). New methodologies for adaptive sliding mode control. *International Journal of Control*, *83*(9), 1907–1919.

Rahnavard, M., Ayati, M., & Hairi Yazdi, M.R. (2018) Robust actuator and sensor fault reconstruction of wind turbine using modified sliding mode observer. *Transactions of the Institute of Measurement and Control*.

Rahnavard, M., Hairi Yazdi, M.R., & Ayati, M. (2017). On the development of a sliding mode observer-based fault diagnosis scheme for a wind turbine benchmark model. *Energy Equipment and Systems*, *5*(1), 13–26.

Ríos, H., Punta, E., & Fridman, L. (2017). Fault detection and isolation for nonlinear non-affine uncertain systems via sliding-mode techniques. *International Journal of Control*, *90*(2), 218–230.

Shtessel, Y., Edwards, C., Fridman, L., & Levant, A. (2014). *Sliding mode control and observation*. New York: Springer.

Su, Y. (2017). Comments on 'A new terminal sliding mode control for robotic manipulators'. *International Journal of Control*, *90*(2), 231–238.

Tan, C.P., Crusca, F., & Aldeen, M. (2008). Extended results on robust state estimation and fault detection. *Automatica*, *44*(8), 2027–2033.

Tan, C.P., & Edwards, C. (2003). Sliding mode observers for robust detection and reconstruction of actuator and sensor faults. *International Journal of Robust and Nonlinear Control*, *13*(5), 443–463.

Tan, C.P., & Edwards, C. (2010). Robust fault reconstruction in uncertain linear systems using multiple sliding mode observers in cascade. *IEEE Transactions on Automatic Control*, *55*(4), 855–867.

Tan, C.P., Yu, X., & Man, Z. (2010). Terminal sliding mode observers for a class of nonlinear systems. *Automatica*, *46*(8), 1401–1404.

Utkin, V. (1992). *Slides modes in control and optimization*. Berlin: Springer Verlag.

Wang, X., Tan, C.P., & Zhou, D. (2017). A novel sliding mode observer for state and fault estimation in systems not satisfying matching and minimum phase conditions. *Automatica*, *79*, 290–295.

Wei, X., & Guo, L. (2009). Composite disturbance-observer-based control and terminal sliding mode control for Non-linear systems with disturbances. *International Journal of Control*, *82*(6), 1082–1098.

Yan, X.-G., & Edwards, C. (2007). Nonlinear robust fault reconstruction and estimation using a sliding mode observer. *Automatica*, *43*, 1605–1614.

Yang, J., & Zhu, F. (2013). Fault detection and isolation design for uncertain nonlinear systems based on full-order, reduced-order and high-order high-gain sliding-mode observers. *International Journal of Control*, *86*(10), 1800–1812.

Yu, S., Yu, X., Shirinzadeh, B., & Man, Z. (2005). Continuous finite-time control for robotic manipulators with terminal sliding mode. *Automatica*, *41*(11), 1957–1964.

Yu, X., & Zhihong, M. (2002). Fast terminal sliding-mode control design for nonlinear dynamical systems. *IEEE Transactions on Circuits and Systems I: Fundamental Theory and Applications*, *49*(2), 261–264.

Zhihong, M., & Yu, X.H. (1997). Terminal sliding mode control of MIMO linear systems. *IEEE Transactions on Circuits and Systems I: Fundamental Theory and Applications*, *44*(11), 1065–1070.

Zuo, Z. (2015). Non-singular fixed-time terminal sliding mode control of non-linear systems. *IET Control Theory & Applications*, *9*(4), 545–552.